Biochemistry

pubs.acs.org/biochemistry Article

Mapping Protein Structural Evolution upon Unfolding

Veena Shankar Avadhani,[†] Supratim Mondal,[†] and Shibdas Banerjee*

Cite This: *Biochemistry* 2022, 61, 303−309 Read Online

ACCESS | Metrics & More | Article Recommendations | Supporting Information

ABSTRACT: In the past, many intensive attempts failed to capture or underestimated the copopulated intermediate conformers from the protein folding/unfolding reaction. We report a promising approach to kinetically trap, resolve, and quantify protein conformers that evolve during unfolding in solution. We conducted acid-induced unfolding of three model proteins (cytochrome *c*, myoglobin, and lysozyme), and the corresponding reaction aliquots upon decreasing the pH were electrosprayed for high field asymmetric waveform ion mobility spectrometry (FAIMS) measurements. The copopulated conformers were resolved, visualized, and quantified by a two-dimensional mapping of the FAIMS output. Contrary to expectations, all the above proteins appeared metamorphic (multiple-folded conformations) at the physiological pH, and cytochrome *c* exhibited an unusual "conformational shuttling" before forming the molten globule state. Thus, in contrast to many previous studies, a wide variety of thermodynamically stable intermediate conformers, including compact, molten globule, and partially unfolded forms, was trapped from solution, probing the unfolding mechanism in detail.

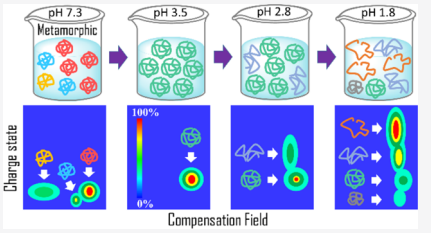

INTRODUCTION

Despite more than half a century of research and tremendous advances in probing techniques, the mechanistic understanding of protein folding/unfolding is still obscure.[1−3] Protein unfolding, misfolding, and aggregation could be the primary cause and consequences of several diseases.[4] Therefore, detecting and quantifying the associated intermediates under equilibrium is paramount in deciphering the pathway(s) that guide a protein to fold or unfold. Often, these intermediates are so sparsely populated that they are challenging to probe by spectroscopic techniques. Moreover, spectroscopic study records the average signal contributed by copopulated conformational ensembles at a specific condition. This spectral signature, if deconvoluted, may underestimate the actual number of conformers involved (Note 1, Supporting Information). Hence, the conformational landscape of a protein could be more complex than previously estimated.[5] In this view, the present work has tracked the protein unfolding process by capturing a wide variety of intermediate species from the associated reaction aliquot in vitro and quantified their abundance during the progress of the unfolding reaction. This approach allowed a thorough investigation of mechanistic pathways of protein unfolding, revealing some previously unrecognized structural features.

MATERIALS AND METHODS

Chemicals. All necessary chemicals and solvents were obtained from commercial sources as mentioned in the Supporting Information.

Sample Preparation. A stock solution of 40 μM of each protein was freshly prepared in 0.5 mM ammonium acetate buffer containing 3% methanol. This stock solution was subsequently diluted using the same buffer whenever required, and then, the protein concentration was determined using UV−Vis absorption at the specific wavelength mentioned in the product information datasheet of the protein (supplied by the commercial source). All FAIMS experiments were performed using 10 μM protein solution in the same buffer, but pH was adjusted by adding hydrochloric acid (HCl) or ammonia wherever required. The pH measurements of the buffer and sample solutions were performed using a highly sensitive pH meter (pH resolution 0.001) as mentioned in the Supporting Information.

Two identical sets of protein solutions were prepared, one for pH measurement and the other for optical spectroscopic studies (UV−Vis, fluorescence, and circular dichroism (CD)). Continuous titration of the protein solution with HCl (from a stock solution) was simultaneously performed on both sets to induce the protein denaturation. A similar approach was followed for the ultraFAIMS/ESI-MS experiment.

Lysozyme reduction was carried out by incubating 100 μM of lysozyme with 10 mM of dithiothreitol (DDT) overnight at 30 °C followed by raising the temperature to 60 °C for 30 min.[6] The above stock solution (DTT was not removed) of the reduced lysozyme was kept back in the incubator at 70 °C after every pH sample preparation for the ultraFAIMS/ESI-MS

Received: November 14, 2021
Revised: December 27, 2021
Published: January 27, 2022

https://doi.org/10.1021/acs.biochem.1c00743
Biochemistry 2022, 61, 303−309

experiment to avoid the formation of disulfide linkages in the protein.

Optical Spectroscopic Measurements. The protein unfolding/conformational change was monitored by Jasco J-1500 CD and Jasco FP-8500 fluorometers along with a UV−Vis spectrophotometer (Agilent Cary series UV−Vis−NIR). Aliquots from the same sample were used for three parallel measurements: UV−Vis, CD, and fluorescence at different pH. A standard 1 min equilibration time was set for the protein solution prepared at different pH before its optical spectroscopic measurement. Further details can be found in the Supporting Information.

Ultrahigh Field Asymmetric Waveform Ion Mobility Spectrometry. The high field asymmetric waveform ion mobility spectrometry (FAIMS) experiment was carried out using a miniaturized ultraFAIMS device (Owlstone Medical Ltd., Cambridge, UK), which was interfaced between a home-built ESI source and a high-resolution mass spectrometer (see below). The above chip-based FAIMS was equipped with an ND chip (Owlstone), which has an analytical gap width of 100 μm, trench length of 97 mm, and a chip thickness of 700 μm. Experiments were carried out at 150 °C chip temperature unless otherwise stated. At 150 °C chip temperature, the dispersion field (DF) can be varied anywhere between 0 to 330 Td. The optimum DF value for separating the protein conformers was investigated by tuning the DF from 30 to 330 Td with a step size of 10 Td, while the compensation field (CF) scan from −10 to +10 Td was set. The CF scan rate was fixed at 0.21 Td/s. An equilibration time of 30 min was allowed for the chip temperature to reach the set value before starting the experiment. After each sample run, a blank of 1:1 water/methanol was electrosprayed to clean the chip and capillaries.

Mass Spectrometry. All mass spectrometry (MS) studies were conducted under identical conditions. The protein solution was electrosprayed at +5 kV potential using a home-built electrospray ionization (ESI) source kept before the ultraFAIMS (Figure S1a). The ESI source was composed of an inner fused silica capillary (100 μm inner diameter and 360 μm outer diameter) and an outer stainless-steel capillary (0.5 mm inner diameter and 1.6 mm outer diameter) placed coaxially. The sample flow rate was fixed at 4 μL/min along with a coaxial sheath gas flow (N_2) at 110 psi backpressure. A spray potential of +5 kV was applied to the stainless-steel needle of the solvent syringe. The distance from the spraying tip to the FAIMS inlet capillary was maintained at 2 cm, and the FAIMS inlet capillary length was 2.5 cm. This allowed the charged droplet to travel enough distance (a total distance of ∼4.5 cm) under the coaxial sheath gas flow to cause analyte desolvation effectively before entering the FAIMS chip. A high-resolution mass spectrometer (Orbitrap Elite Hybrid Ion Trap-Orbitrap Mass Spectrometer, ThermoFisher Scientific, Newington, NH, USA) was coupled to the ultraFAIMS to detect the transmitted ions. We maintained the MS inlet capillary temperature at 300 °C and the S-lens RF level at 69.5% under positive ion mode. The mass spectra were recorded over a range of m/z 700−4000 at a resolution of 60,000. The data acquisition was performed for 1.62 min (same as the CF scan time) using XCalibur software (ThermoFisher Scientific).

Data Analysis. Optical spectroscopic and mass spectrometric data were extracted in Microsoft Excel and plotted using Origin 2020b software. The protein ion signal intensities were measured from the FAIMS spectrum (ion chronogram) at a 0.04 min step size and organized in a matrix of charge states versus time points to make the contour plots (FAIMS/ESI-MS mapping). The intensity values in the matrix were handpicked manually from the high-resolution XCalibur file (details in the Supporting Information). The conversion of time scale (from the FAIMS output) to CF scale was carried out using a conversion template provided by Owlstone Medical Pvt. Ltd. on their website.

Relative Quantitation of Conformers. We determined the fractional abundance of conformers as a function of pH from the FAIMS/ESI-MS data for the quantitative estimation of gradual conformational change. The abundance of a protein conformation can be represented by the summation of signal intensities of all the charge states belonging to the CSD of that conformer.[7] Therefore, we extracted the ion signal intensities (absolute) of the CSD at the specific CF (see Figure S4 as an example) of different conformers observed in the FAIMS/ESI-MS map to calculate their relative (fractional) abundance. When two or more nearby CSDs tend to overlap, we deconvoluted the corresponding CSD data presenting the combination of multiple Gaussian curves (CSDs) and then picked up the intensity values from the resulting (deconvoluted) Gaussian curves (see Figure S7 as a typical example) to estimate the fractional abundance of the associated conformers. It should be noted that this quantification, although it may not be highly accurate, is a ballpark estimate of the copopulated conformational ensembles, which is otherwise difficult to decipher by an alternate technique.

RESULTS AND DISCUSSION

Figure 1 shows our experimental workflow involving ultrahigh field asymmetric waveform ion mobility spectrometry (ultra-

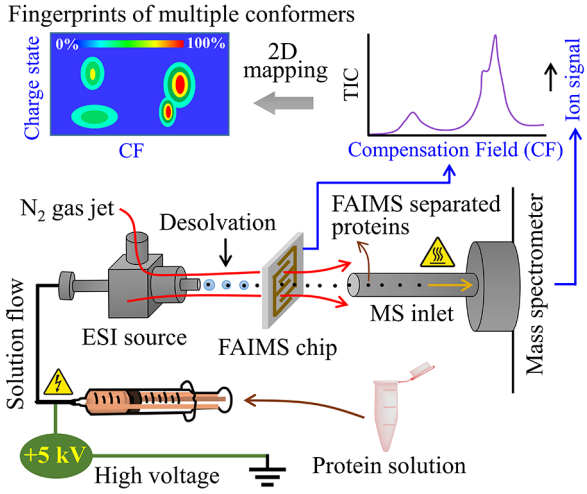

Figure 1. ESI-ultraFAIMS-MS experimental set-up to capture, separate, and detect copopulated protein conformers in solution.

FAIMS)[8,9] coupled to mass spectrometry (MS) employed in this study (see Note 2 in the Supporting Information and Figure S1 for details).

We followed the acid-induced unfolding/structural changes of three proteins (cytochrome *c*, myoglobin, and lysozyme; Figure S2), which are the most extensively studied model proteins for conformational changes. While gradually lowering the pH of the protein solution in steps, we pipetted out a small volume (50 μL) of the reaction aliquot in each stage for

https://doi.org/10.1021/acs.biochem.1c00743
Biochemistry 2022, 61, 303−309

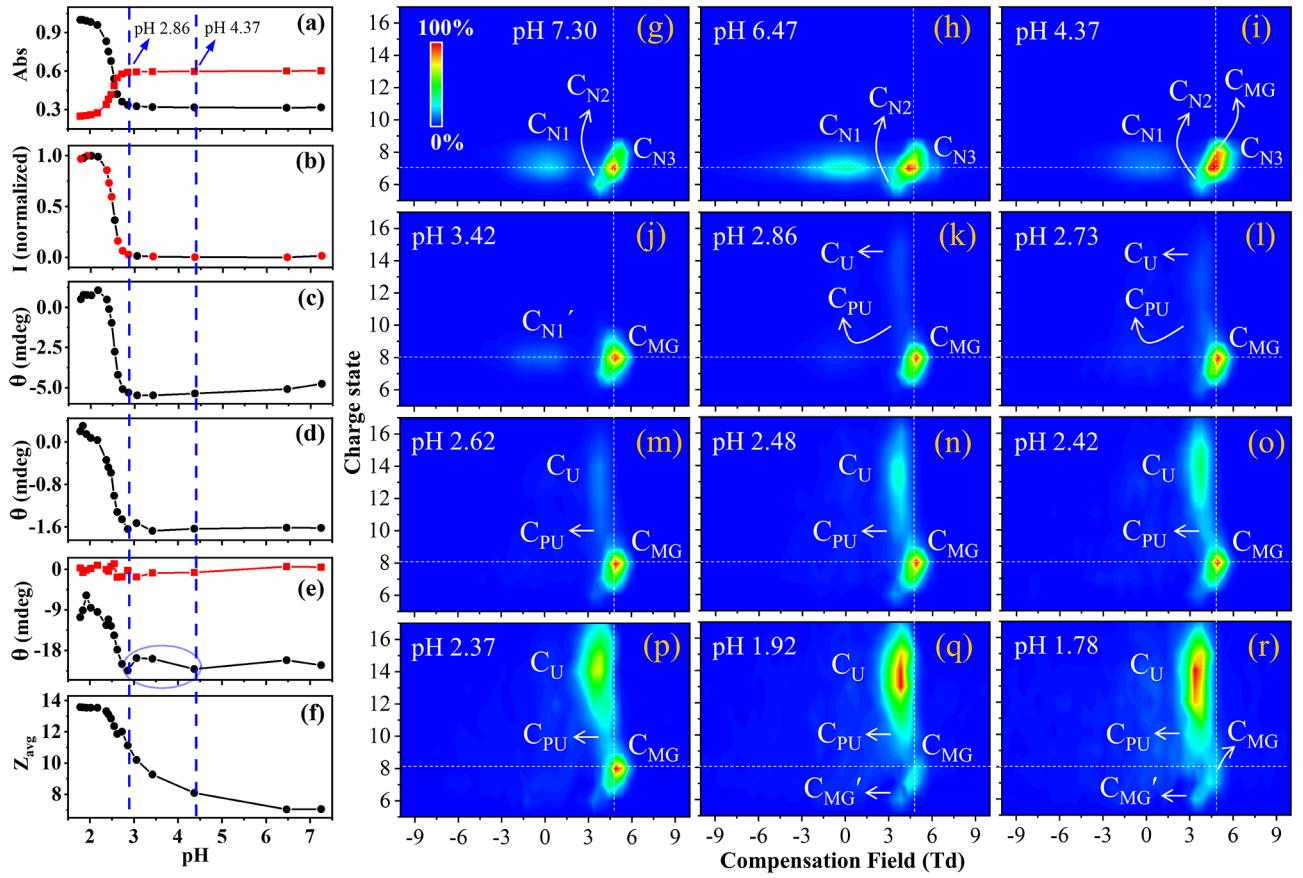

Figure 2. Monitoring acid-induced unfolding of horse heart cytochrome *c* by (a) Soret absorptions at 409 nm (red dots) and 394 nm (black dots), (b) Trp fluorescence emission at 340 nm upon excitation at 280 nm, (c) Soret CD band at 418 nm, (d) CD signal at 289 nm for the breakdown of the tertiary structure, (e) CD signals at 222 nm (black dots) and 208 nm (red dots) for effect on the secondary structure, and (f) average charge state calculated from the ESI-MS data (FAIMS off) recorded at different pH levels of the protein aliquot (see Materials and Methods). Right palettes (g–r) present the ultraFAIMS/ESI-MS mapping of 10 μM horse heart cytochrome *c* at varying pH (red dots in (b)), showing the charge state distribution as a function of compensation field applied to the FAIMS chip kept under a 330 Td dispersion field (optimized) and 150 °C temperature. The most intense ion signal is normalized to 100% in each palette drawn as a false-color map (inset of (g)) along with the interpolation between the discrete charge states for viewing convenience. Metamorphic conformers (C_{N1}, C_{N2}, and C_{N3}) transitioned to unfolded conformer (C_U) via molten globule (C_{MG}) and partially unfolded (C_{PU}) states (Figure 3). The electric field is expressed in Townsends (Td; see Note 2 in the Supporting Information).

directly injecting to a home-built electrospray ionization (ESI) source that rapidly transferred the protein species from solution to the gas phase. The pneumatic force carried the gaseous protonated proteins, thus formed through the orthogonally placed ultraFAIMS chip consisting of miniaturized electrodes. While passing through this chip, protein conformers were separated based on their differential mobilities under the influence of alternating low and high electric fields (dispersion field, DF) in combination with a direct current electric field called compensation field (CF).[10] Thus, different conformers were separated, transmitted from the chip on ramping the CF, and then detected by a mass spectrometer (Note 3, Supporting Information).[11] The entire process, including gaseous protein formation from electrospray droplets,[12] FAIMS separation,[8] and mass spectrometric detection takes a few milliseconds (Note 4, Supporting Information). In contrast to many previous reports,[13−18] we evaluated the ESI-FAIMS-MS data to resolve and visualize fingerprints of different protein conformers in solution based on their differential mobilities (related to CF) and charge state distributions (CSDs), which were plotted in two dimensions (2D) as the CSD vs CF contour plot (Figure 1; see Materials and Methods for details). The unfolding of protein results in expanding its solvent-accessible surface area, leading to an increase in CSD.[19,20] Although multiple conformers could contribute to a monomodal CSD, we distinguished those conformers based on their elution at different CF. It should be noted that the residence time of the analyte molecule in the ultraFAIMS chip is less than 250 μs.[8] At a specific CF, the CSD reflects the memory of the corresponding protein conformer intercepted from the solution irrespective of the subtle conformational fluctuation (tertiary structure) that may happen in the gas phase on a millisecond timescale (Notes 5 and 6, Supporting Information).

Study on Cytochrome *c*. We began our investigation using horse heart cytochrome *c* (Cyt. *c*), a small heme protein (~12.4 kDa) that participates in the electron-transfer process in mitochondria. The unfolding reaction was performed by gradually adding hydrochloric acid (HCl) to the protein solution in 0.5 mM ammonium acetate buffer containing 3% methanol. We selected this ESI-MS-friendly buffer as both ammonium acetate and a trace amount of methanol is known to enhance and stabilize the signal intensity of the protonated species.[20,21] The unfolding study was subjected to four parallel

https://doi.org/10.1021/acs.biochem.1c00743
Biochemistry 2022, 61, 303−309

measurements: UV−Vis, fluorescence, circular dichroism-(CD), and MS (Figure 2). Optical spectroscopic data (Figure 2a−e and Note 7, Supporting Information) indicated pH 2.86 as the onset acidic pH for Cyt. *c* unfolding. Based on these results, 12 pH points of interest (red dots in Figure 2b) that covered the entire unfolding landscape (Figure 2) were replicated for the ultraFAIMS-MS study.

The performance of ultraFAIMS on resolving Cyt. *c* conformers at a typical pH of 6.47 (no HCl added) was first optimized using a CF/DF sweep that resulted in maximum resolution at 330 Td DF (Figure S3). Figure 2g−r presents the ultraFAIMS/MS mapping of Cyt. *c* conformational evolution upon acid-induced unfolding (see Materials and Methods). Each conformer and its abundance are manifested by the characteristic CSD at a specific CF in the FAIMS/MS palette. Interestingly, at around the physiological pH, Cyt. *c* was found to be a metamorphic protein,[22−25] adopting three distinct compact native (or native-like) conformers (C_{N1}, C_{N2}, and C_{N3}) in equilibrium (Figure 2g).[26] Hackenbrock and co-workers[27] have shown earlier that although in the mitochondrial environment, cytochrome *c* exists in multiple conformations. While C_{N3} was found to be the dominant native conformer, the narrower CSD of C_{N2} suggests it to be more compact than C_{N1} or C_{N3} (Figure S4). On reducing the solution pH up to 4.37, the relative abundance of the C_{N1} conformer initially increases and then decreases, indicating an equilibrium-mediated "conformational shuttling" between C_{N1} and C_{N3} (Figure 2g−i). This shuttling behavior was more evident at 75 °C chip temperature (Figure S8a−c). While the exact reason for this conformational shuttling is currently uncertain, this phenomenon appears to be without precedent and needs to be investigated further in the future. Moreover, C_{N2} also transformed into C_{N3} upon lowering of the pH. Further pH reduction developed swelled (C_{N1}') and molten globule[28] (C_{MG}) conformers as indicated by the slight shift of the CSD center from +7 to +8 (Figure 2j). This result also suggested that the Cyt. *c* molten globule state is slightly larger (~8% difference in radius) than the native state (Note 8, Supporting Information and Table S1).[29]

We traced the partially unfolded (C_{PU}, CSD centering at +10) the unfolded (C_U, CSD centering at +14) conformers, which started forming from pH 2.86, which is the onset acidic pH for Cyt. *c* unfolding also observed in the corresponding optical spectroscopic data (Figure 2a−e). This result makes us believe that solution conformers are kinetically trapped during the electrospraying of proteins into the gas phase, which the Clemmer group[30] has also reviewed lately. The abundance of the unfolded conformer was found to be the highest with the simultaneous appearance of another compact molten globule state (C_{MG}') in the vicinity of pH 2 (Figure 2q,r and Figures S5 and S6), which is consistent with the earlier observation by the Fink group.[31] Our data (Figures S5 and S6) suggest that C_{MG}' is more compact than C_{MG} and is possibly derived from the C_{MG} by binding chloride anions, which minimizes the intramolecular charge repulsion. This chloride adduct formation is prominent in the mass spectra recorded at low pH (Figures S5−6).

Based on the above observations, Figure 3a presents the structural transition of metamorphic Cyt. *c* during the acid-induced unfolding process. All the associated precursors, intermediates, and product conformers (total of 8) were FAIMS-separated and detected by the MS (Figure 2). The contour plotting (Figure 2g−r) also enabled us to predict the

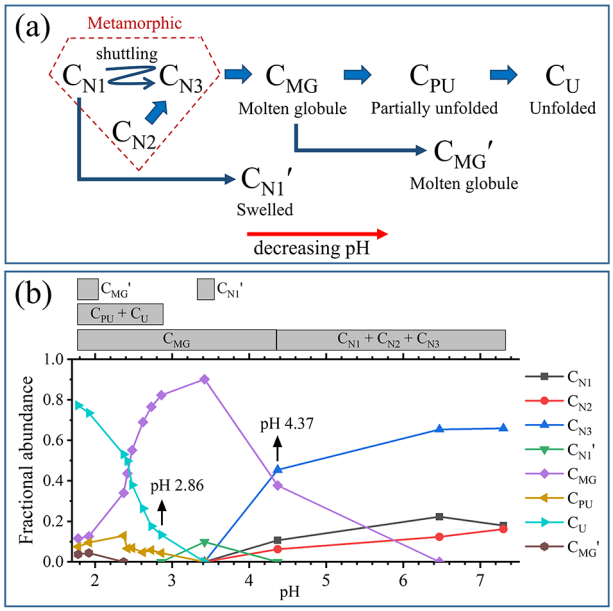

Figure 3. (a) Schematic presentation of acid-induced conformational transition of cytochrome *c* as deciphered by ultraFAIMS/ESI-MS mapping (Figure 2g−r). (b) Fractional abundance of different conformers upon decreasing the pH of the cytochrome *c* solution. The pH ranges over which different conformers are observed (Figure 2g−r) are indicated by horizontal bars on the top of the graph.

fractional abundance of each conformer in solution as a function of pH (Figure 3b), which is otherwise difficult to quantitate by other techniques. Figure S7 presents a typical deconvolution process[7,32] to resolve CSDs of two or more overlapping conformers at a given CF to quantify them.[7] It should be noted that all detected conformers are thermodynamically stable as they exist over a wide range of pH (Figure 3b). Figure 3b shows that molten globule and unfolded conformers start forming at pH levels of 4.37 and 2.86, respectively. This can also be attributed to the slight fluctuation of secondary CD bands observed between these two pHs (circled in Figure 2e). These trends are even followed at 75 °C FAIMS chip temperature (Figure S8−S10), although with a slight variation of resolution and sensitivity caused by the heating effect in the FAIMS stage.

After experiencing the evaporative cooling effect (during droplet evolution), the electrospray-generated bare protein molecules might not be heated much in the ultraFAIMS stage (thermal and field heating)[13,33] to cause dramatic structural alteration since we noted an overall good agreement between solution (optical) and ultraFAIMS studies (Figure 2). However, subtle conformational change by ultraFAIMS heating cannot be completely ignored.[11]

Study on Myoglobin. We also monitored acid-induced structural changes of horse-heart myoglobin (Mb), a non-covalently bound heme protein. The optical spectroscopic studies of the solution phase (Figure S11 and Note 9 in the Supporting Information) corresponded well with the ultraFAIMS/ESI-MS mapping (Figure S12) at the optimum DF (Figure S13). The MS data suggested that the gradual reduction of solution pH results in heme release from the holo form (holo-Mb), which starts and completes in the vicinity of pH 4.0 and 3.3, respectively (Figures S14 and S15), leading to the apo-form (apo-Mb), which consistent with the optical measurements (Figure S11). Our 2D mapping method

https://doi.org/10.1021/acs.biochem.1c00743
Biochemistry 2022, 61, 303−309

facilitates selective analysis of the holo- and apo-forms due to their different m/z values. At the physiological pH, three myoglobin conformers (metamorphic M_{N1}, M_{N2}, and M_{N3}) were resolved (Figure S16), although one among those was found to be the dominant form (M_{N3}). A prior study[34] revealed that the mechanism of acid denaturation of holo-Mb proceeds through a distended holo-state before forming the apo-Mb. In another study,[35] this distended holo-Mb with insignificant changes in secondary structure but with perturbed tertiary structure was attributed to the molten globule state of holo-Mb that was obtained in the presence of polyethylene glycol (denaturant). In our study, we could also trace this molten globule form (Figure S12d–i), which is slightly larger (ΔR ~9.5%, Table S1) than the native state, that started forming from pH 4.79 and continued to exist until holo-Mb vanished (transformed completely into apo-Mb) below pH 3.35. (Figures S12i and S15). Surprisingly, we also detected, albeit less in quantity, the partially and fully unfolded forms of holo-Mb (heme still attached to the protein!) at pH 3.35 (M_{PU} and M_U; Figure S12i) before it was completely converted to apo-Mb. Many past observations suggested that the nature of apo-Mb at pH 4 is similar to a molten globule state.[36−40] Therefore, we annotated the apo-Mb conformers observed at pH 3.99 as molten globules (A_{MG1} and A_{MG2}, Figure S12j), and corresponding CSDs were also similar to that of the molten globule holo-Mb (M_{MG}; Figure S12g).

In an earlier report, Dobo and Kaltashov[32] had deconvoluted the CSD pattern obtained from the ESI-MS of apo-Mb in the pH range of 2.5 to 8.6 to propose the presence of four different conformers. These conformers were N (native-like), I (pH 4 intermediate), E (extended conformer), and U (unfolded state). Our results also comply with the same theory, but some notable differences are present, as discussed below.

The intermediate form I corresponds to the molten globule conformer that accumulates at pH 4. Unlike their report, we resolved the intermediate species at this pH and detected the presence of two metamorphic apo-conformers, A_{MG1} and A_{MG2}, as shown in Figure S12j. According to Goto and Fink,[41] the intermediate state at this pH has a 60% higher hydrodynamic radius compared to the native form. This was mainly attributed to the unfolding of the B and E helices.[42] Thus, the two isoforms observed here may be due to the different unfolding patterns of these helices. We traced the formation of further partially unfolded conformers A_{PU1} and A_{PU2} emerging from A_{MG1} and A_{MG2}, respectively, as shown in Figures S12k and S17. While Dobo and Kaltashov[32] presumed conformer "E" as the molten globule state (prominent at pH 3.5 in their study), this state seems relatable to A_{PU1} in our case (Figure S12m). Further reduction of pH led unfolded conformer A_U (Figure S12n–r) along with another partially unfolded state (A_{PU3}) that started forming below pH 3.3 (Figures S12p–r and S18), possibly because of chloride adduct formation (similar to Cyt. c).

Based on all these observations, we have proposed stepwise unfolding mechanisms for both holo-Mb and apo-Mb (Figure 4a,b) along with the fractional abundance of the conformers throughout the unfolding landscape (Figures S19 and S20). Literature reports[19,43] on the acid-induced unfolding of apo-Mb using optical spectroscopy and ESI-MS suggest a noncooperative unfolding process that would involve multiple interconverting conformations. Our observations from this study are also in accordance with those proposed models.

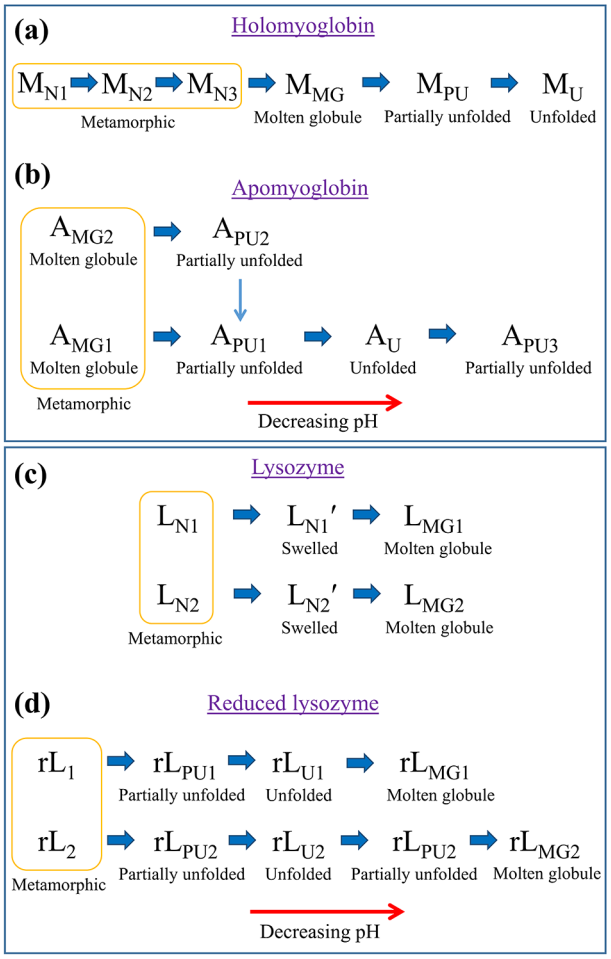

Figure 4. Schematic presentation of acid-induced conformational transitions of (a) holomyoglobin, (b) apomyoglobin, (c) lysozyme, and (d) reduced lysozyme as deciphered by their ultraFAIMS/ESI-MS mappings (Figure S12a–i, S12j–r, S23, and S29, respectively).

Study on Lysozyme. Analogous studies were also performed on the hen egg lysozyme (Lys) for both native (Figures S21–S26) and disulfide-reduced (Figures S27–S31) forms (Note 10, Supporting Information). As expected,[44] native lysozyme (nonreduced-Lys) did not show any significant unfolding owing to its disulfide-rendered robustness (Figure S23). However, we report minor tertiary structure aberrations based on optical probe features and 2D mass spectrometric maps. Figure S21a suggests a two-step transition of nonreduced-Lys during acid-induced uncoiling, and the corresponding changes are also visible in palette plots (Figure S23). The contour plots show the emergence of two swelled conformers L_{N1}' and L_{N2}' from the native conformers L_{N1} and L_{N2} (metamorphic), respectively (Figure S23e–g). These new conformers tend to show 9.2 and 6.8% expansion in radii compared with their precursors (Table S1). pH 2.12 and pH 1.82 mark the formation of compact molten globule states, namely, L_{MG1} and L_{MG2} (Figure S23k,l). This feature agrees with Lee and Kim's finding[44] that confirmed the suppression of unfolding and triggering of refolding by HCl at low pH. Indeed, the molten globule states L_{MG1} and L_{MG2} seem to shrink with radius changes of 10.1 and 7.1% from their respective native counterparts (Table S1). The optical probes also reconciled well with these changes below pH 2.12 (Figure S21a–c).

https://doi.org/10.1021/acs.biochem.1c00743
Biochemistry 2022, 61, 303−309

On the contrary, disulfide-reduced Lys is free from any strong tertiary structural constraints, and hence, widespread distributions of acid-unfolded conformers were evident in the 2D FAIMS/MS maps (Figure S29). The three stages of significant transitions in the map correlate with the other spectroscopic results (Figure S27). The native conformers rL_1 and rL_2 transformed into unfolded rL_{U1} and rL_{U2} via partially unfolded states rL_{PU1} and rL_{PU2}, respectively (Figure 4d). Analogous to other proteins considered in this study, reduced-Lys also experienced refolding of the polypeptide chain in the vicinity of pH 2 to form compact molten globule conformers (rL_{MG1} and rL_{MG2}) due to chloride adduct formation, which was evident in the mass spectra (Figure S30). These results outperform the earlier measurements in resolving Lys conformers obtained from the FAIMS peak deconvolution method.[45]

Based on these findings, we propose the mechanistic routes of stepwise structural changes for both Lys (Figure 4c) and reduced-Lys (Figure 4d) along with the fractional abundance of the copopulated conformers (Figures S26 and S31).

In summary, all these results substantiate a straightforward but powerful approach to intercept, resolve, and quantitatively measure protein conformers during the progress of unfolding reactions in microscale. Although conducted in vitro, this study provides insight into the nature and complexity of protein folding/unfolding pathways in vivo.

CONCLUSIONS

Protein conformational change is a fundamental and ubiquitous process in the biological system. The malfunctioning of a protein is often linked to the aberration of its shape, which might cause severe consequences including the development of a disease. Therefore, it is highly desirable to kinetically trap and measure the protein conformation upon changing its environment. We applied ultrahigh field asymmetric waveform ion mobility spectrometry coupled to mass spectrometry to rapidly intercept copopulated protein conformers in solution to track and visualize unfolding routes of some model proteins. This development also allows the quantitative estimation of different intermediate conformers at a specific time or condition and presents some previously unrecognized structural features associated with protein unfolding.

ASSOCIATED CONTENT

Supporting Information

The Supporting Information is available free of charge at https://pubs.acs.org/doi/10.1021/acs.biochem.1c00743.

Supplementary notes and tables; materials and methods; FAIMS and mass spectral data; quantitative estimation of different copopulated conformers (PDF)

Accession Codes

UniProt protein IDs: CYC: P00004 MB: P68082 LYZ: P00698

AUTHOR INFORMATION

Corresponding Author

Shibdas Banerjee − *Department of Chemistry, Indian Institute of Science Education and Research Tirupati, Tirupati 517507, India;* orcid.org/0000-0002-3424-8157; Email: shibdas@iisertirupati.ac.in

Authors

Veena Shankar Avadhani − *Department of Chemistry, Indian Institute of Science Education and Research Tirupati, Tirupati 517507, India*

Supratim Mondal − *Department of Chemistry, Indian Institute of Science Education and Research Tirupati, Tirupati 517507, India*

Complete contact information is available at: https://pubs.acs.org/10.1021/acs.biochem.1c00743

Author Contributions

†V.S.A. and S.M. contributed equally to this work.

Author Contributions

S.B. designed and supervised the research. V.S.A. and S.M. performed experiments. All authors analyzed data and wrote the paper.

Notes

The authors declare no competing financial interest.

ACKNOWLEDGMENTS

Authors thank SERB, India, for supporting this work (grant numbers SB/S2/RJN-130/2017 and ECR/2018/001268).

REFERENCES

(1) Dill, K. A.; Ozkan, S. B.; Shell, M. S.; Weikl, T. R. The protein folding problem. *Annu. Rev. Biophys.* **2008**, *37*, 289−316.

(2) Finkelstein, A. V.; Badretdin, A. J.; Galzitskaya, O. V.; Ivankov, D. N.; Bogatyreva, N. S.; Garbuzynskiy, S. O. There and back again: Two views on the protein folding puzzle. *Phys. Life. Rev.* **2017**, *21*, 56−71.

(3) Englander, S. W.; Mayne, L. The nature of protein folding pathways. *Proc. Natl. Acad. Sci. U. S. A.* **2014**, *111*, 15873−15880.

(4) Soto, C.; Pritzkow, S. Protein misfolding, aggregation, and conformational strains in neurodegenerative diseases. *Nat. Neurosci.* **2018**, *21*, 1332−1340.

(5) Gianni, S.; Freiberger, M. I.; Jemth, P.; Ferreiro, D. U.; Wolynes, P. G.; Fuxreiter, M. Fuzziness and Frustration in the Energy Landscape of Protein Folding, Function, and Assembly. *Acc. Chem. Res.* **2021**, *54*, 1251−1259.

(6) Konermann, L.; Douglas, D. J. Unfolding of proteins monitored by electrospray ionization mass spectrometry: a comparison of positive and negative ion modes. *J. Am. Soc. Mass Spectrom.* **1998**, *9*, 1248−1254.

(7) Borysik, A. J. H.; Radford, S. E.; Ashcroft, A. E. Co-populated conformational ensembles of beta2-microglobulin uncovered quantitatively by electrospray ionization mass spectrometry. *J. Biol. Chem.* **2004**, *279*, 27069−27077.

(8) Shvartsburg, A. A.; Smith, R. D.; Wilks, A.; Koehl, A.; Ruiz-Alonso, D.; Boyle, B. Ultrafast differential ion mobility spectrometry at extreme electric fields in multichannel microchips. *Anal. Chem.* **2009**, *81*, 6489−6495.

(9) Shvartsburg, A. A.; Tang, K.; Smith, R. D.; Holden, M.; Rush, M.; Thompson, A.; Toutoungi, D. Ultrafast differential ion mobility spectrometry at extreme electric fields coupled to mass spectrometry. *Anal. Chem.* **2009**, *81*, 8048−8053.

(10) Kolakowski, B. M.; Mester, Z. Review of applications of high-field asymmetric waveform ion mobility spectrometry (FAIMS) and differential mobility spectrometry (DMS). *Analyst* **2007**, *132*, 842−864.

(11) Cooper, H. J. To What Extent is FAIMS Beneficial in the Analysis of Proteins? *J. Am. Soc. Mass Spectrom.* **2016**, *27*, 566−577.

(12) Banerjee, S.; Mazumdar, S. Electrospray Ionization Mass Spectrometry: A Technique to Access the Information beyond the Molecular Weight of the Analyte. *Int. J. Anal. Chem.* **2012**, *2012*, 282574.

(13) Hale, O. J.; Illes-Toth, E.; Mize, T. H.; Cooper, H. J. High-Field Asymmetric Waveform Ion Mobility Spectrometry and Native Mass Spectrometry: Analysis of Intact Protein Assemblies and Protein Complexes. *Anal. Chem.* **2020**, *92*, 6811−6816.
(14) Purves, R. W.; Barnett, D. A.; Guevremont, R. Separation of protein conformers using electrospray-high field asymmetric waveform ion mobility spectrometry-mass spectrometry. *Int. J. Mass Spectrom.* **2000**, *197*, 163−177.
(15) Robinson, E. W.; Williams, E. R. Multidimensional separations of ubiquitin conformers in the gas phase: relating ion cross sections to H/D exchange measurements. *J. Am. Soc. Mass Spectrom.* **2005**, *16*, 1427−1437.
(16) Voronina, L.; Rizzo, T. R. Spectroscopic studies of kinetically trapped conformations in the gas phase: the case of triply protonated bradykinin. *Phys. Chem. Chem. Phys.* **2015**, *17*, 25828−25836.
(17) Shvartsburg, A. A. Ultrahigh-Resolution Differential Ion Mobility Separations of Conformers for Proteins above 10 kDa: Onset of Dipole Alignment? *Anal. Chem.* **2014**, *86*, 10608−10615.
(18) Shvartsburg, A. A.; Smith, R. D. Separation of Protein Conformers by Differential Ion Mobility in Hydrogen-Rich Gases. *Anal. Chem.* **2013**, *85*, 6967−6973.
(19) Konermann, L.; Douglas, D. J. Equilibrium unfolding of proteins monitored by electrospray ionization mass spectrometry: distinguishing two-state from multi-state transitions. *Rapid Commun. Mass Spectrom.* **1998**, *12*, 435−442.
(20) Konermann, L.; Douglas, D. J. Acid-Induced Unfolding of Cytochrome c at Different Methanol Concentrations: Electrospray Ionization Mass Spectrometry Specifically Monitors Changes in the Tertiary Structure. *Biochemistry* **1997**, *36*, 12296−12302.
(21) Przybylski, M.; Glocker, M. O. Electrospray Mass Spectrometry of Biomacromolecular Complexes with Noncovalent Interactions—New Analytical Perspectives for Supramolecular Chemistry and Molecular Recognition Processes. *Angew. Chem. Int. Ed. Engl.* **1996**, *35*, 806−826.
(22) Dishman, A. F.; Volkman, B. F. Unfolding the Mysteries of Protein Metamorphosis. *ACS Chem. Biol.* **2018**, *13*, 1438−1446.
(23) Lella, M.; Mahalakshmi, R. Metamorphic Proteins: Emergence of Dual Protein Folds from One Primary Sequence. *Biochemistry* **2017**, *56*, 2971−2984.
(24) Murzin, A. G. Metamorphic Proteins. *Science* **2008**, *320*, 1725−1726.
(25) Yadid, I.; Kirshenbaum, N.; Sharon, M.; Dym, O.; Tawfik, D. S. Metamorphic proteins mediate evolutionary transitions of structure. *Proc. Natl. Acad. Sci. U. S. A.* **2010**, *107*, 7287−7292.
(26) Vila, J. A. Thoughts on the Protein's Native State. *J. Phys. Chem. Lett.* **2021**, *12*, 5963−5966.
(27) Cortese, J. D.; Voglino, A. L.; Hackenbrock, C. R. Multiple Conformations of Physiological Membrane-Bound Cytochrome c. *Biochemistry* **1998**, *37*, 6402−6409.
(28) Pletneva, E. V.; Gray, H. B.; Winkler, J. R. Nature of the Cytochrome c Molten Globule. *J. Am. Chem. Soc.* **2005**, *127*, 15370−15371.
(29) Nakamura, S.; Seki, Y.; Katoh, E.; Kidokoro, S.-i. Thermodynamic and Structural Properties of the Acid Molten Globule State of Horse Cytochrome c. *Biochemistry* **2011**, *50*, 3116−3126.
(30) Raab, S. A.; El-Baba, T. J.; Laganowsky, A.; Russell, D. H.; Valentine, S. J.; Clemmer, D. E. Protons Are Fast and Smart; Proteins Are Slow and Dumb: On the Relationship of Electrospray Ionization Charge States and Conformations. *J. Am. Soc. Mass Spectrom.* **2021**, *32*, 1553−1561.
(31) Goto, Y.; Calciano, L. J.; Fink, A. L. Acid-induced folding of proteins. *Proc. Natl. Acad. Sci. U. S. A.* **1990**, *87*, 573−577.
(32) Dobo, A.; Kaltashov, I. A. Detection of Multiple Protein Conformational Ensembles in Solution via Deconvolution of Charge-State Distributions in ESI MS. *Anal. Chem.* **2001**, *73*, 4763−4773.
(33) Robinson, E. W.; Shvartsburg, A. A.; Tang, K.; Smith, R. D. Control of ion distortion in field asymmetric waveform ion mobility spectrometry via variation of dispersion field and gas temperature. *Anal. Chem.* **2008**, *80*, 7508−7515.
(34) Konermann, L.; Rosell, F. I.; Mauk, A. G.; Douglas, D. J. Acid-induced denaturation of myoglobin studied by time-resolved electrospray ionization mass spectrometry. *Biochemistry* **1997**, *36*, 6448−6454.
(35) Parray, Z. A.; Shahid, S.; Ahmad, F.; Hassan, M. I.; Islam, A. Characterization of intermediate state of myoglobin in the presence of PEG 10 under physiological conditions. *Int. J. Biol. Macromol.* **2017**, *99*, 241−248.
(36) Kataoka, M.; Nishii, I.; Fujisawa, T.; Ueki, T.; Tokunaga, F.; Goto, Y. Structural characterization of the molten globule and native states of apomyoglobin by solution X-ray scattering. *J. Mol. Biol.* **1995**, *249*, 215−228.
(37) Lin, L.; Pinker, R. J.; Forde, K.; Rose, G. D.; Kallenbach, N. R. Molten globular characteristics of the native state of apomyoglobin. *Nat. Struct. Biol.* **1994**, *1*, 447−452.
(38) Yao, J.; Chung, J.; Eliezer, D.; Wright, P. E.; Dyson, H. J. NMR Structural and Dynamic Characterization of the Acid-Unfolded State of Apomyoglobin Provides Insights into the Early Events in Protein Folding. *Biochemistry* **2001**, *40*, 3561−3571.
(39) Griko, Y. V.; Privalov, P. L.; Venyaminov, S. Y.; Kutyshenko, V. P. Thermodynamic study of the apomyoglobin structure. *J. Mol. Biol.* **1988**, *202*, 127−138.
(40) Griko, Y. V.; Privalov, P. L. Thermodynamic Puzzle of Apomyoglobin Unfolding. *J. Mol. Biol.* **1994**, *235*, 1318−1325.
(41) Goto, Y.; Fink, A. L. 1 Acid-induced folding of heme proteins. *Methods Enzymol.* **1994**, *232*, 3−15.
(42) Hughson, F. M.; Wright, P. E.; Baldwin, R. L. Structural characterization of a partly folded apomyoglobin intermediate. *Science* **1990**, *249*, 1544−1548.
(43) Goto, Y.; Fink, A. L. Phase diagram for acidic conformational states of apomyoglobin. *J. Mol. Biol.* **1990**, *214*, 803−805.
(44) Lee, J. W.; Kim, H. I. Investigating acid-induced structural transitions of lysozyme in an electrospray ionization source. *Analyst* **2015**, *140*, 661−669.
(45) Robinson, E. W.; Sellon, R. E.; Williams, E. R. Peak deconvolution in high-field asymmetric waveform ion mobility spectrometry (FAIMS) to characterize macromolecular conformations. *Int. J. Mass Spectrom.* **2007**, *259*, 87−95.

https://doi.org/10.1021/acs.biochem.1c00743
Biochemistry 2022, 61, 303−309